Polymer Degradation and Stability 95 (2010) 870–879

Contents lists available at ScienceDirect

Polymer Degradation and Stability

journal homepage: www.elsevier.com/locate/polydegstab

Effect of carbon nanotubes and montmorillonite on the flammability of epoxy nanocomposites

Sameer S. Rahatekar [a,1], Mauro Zammarano [a], Szabolcs Matko [a], Krzysztof K. Koziol [b], Alan H. Windle [b], Marc Nyden [a], Takashi Kashiwagi [a], Jeffrey W. Gilman [a,*]

[a] Building and Fire Research Laboratory, National Institute of Standards and Technology, Gaithersburg, MD 20899, USA
[b] University of Cambridge, Materials Science and Metallurgy, Cambridge CB2 3QZ, UK

ARTICLE INFO

Article history:
Received 25 June 2009
Received in revised form
15 December 2009
Accepted 5 January 2010
Available online 14 January 2010

Keywords:
Carbon nanotubes
Montmorillonite
Nanocomposites
Flammability
Epoxy
Rheology

ABSTRACT

Addition of just 0.0025 mass fraction of highly aligned multiwall carbon nanotubes (MWCNTs) showed a 45% reduction in the peak mass loss rate (PMLR) during gasification of epoxy/MWCNT composites; this 45% decrease in PMLR at such a low loading (0.0025mass fraction) of MWCNTs, is much better than that reported previously with either MWCNTs (0.02 mass fraction) or SWCNTs (0.005 mass fraction). We attribute this effect to the use of highly aligned MWCNTs which easily exfoliate, or debundle, using high shear mixing. In addition, 0.005 mass fraction MWCNTs showed significant reduction in the *initial* mass loss rate as compared to other epoxy/MWCNT, epoxy montmorillonite (MMT) and pure epoxy samples. Reduced PMLR was also observed for epoxy/MMT nanocomposites, but required much higher MMT content. The epoxy/MWCNTs composites residue/char integrity (no visible cracks on the char surface of MWCNTs/epoxy samples) appeared to be superior to that for epoxy/MMT samples. The rheological characterization of the epoxy composites was carried out in order to study the effect of nanoparticle network formation on the rheological properties and flammability. Significant increase in thermal conductivity (k) was observed for epoxy/MWCNTs composite with high loadings of MWCNTs. This gasification mass loss behavior of the nanocomposites was investigated using a model that combines a continuum description of the transport of thermal energy with Ahrrenius kinetics for the decomposition of the polymer. The enhanced thermal conductivity for the epoxy/MWCNT composites appears to be responsible for the initial mass loss reduction.

1. Introduction

Pioneering work by a number of groups has shown that well dispersed montmorillonite (MMT) [1] or MWNTs [2,3] in a polymer matrix can significantly reduce the flammability of a wide range of polymers. It is proposed that anisotropic nanoparticles, such as nanoclays and carbon nanotubes, form a protective layer on the surface of a polymer [2,4,5] during combustion or pyrolysis. This protective layer shields the underlying polymer from the external heat flux, and reduces the volatilization rate of fuel gases by inhibiting bubble escape in the polymer melt.

Wheras a number of detailed studies have elucidated the important controlling factors in the mechanism of flame retardancy for both carbon nanotubes [2–10] and MMT [1,11,12], no direct comparison of these two nanoadditives based flame retardant system has been made in the same thermoset resin system exposed to the same fire-like conditions. Here, a direct comparison of flammability (using nitrogen gasification) of epoxy MWCNT and epoxy/MMT composites is presented.

The aim of the present work is to study and compare the gasification of epoxy/MWCNTs and epoxy/MMT composites. Modeling of the gasification process of epoxy/MWCNTs as well as epoxy/MMT composites is conducted in order to understand and compare the mass loss rate (MLR) curves for both type of composites. Previously, Kashiwagi et al. [2] showed that network formation of nanoparticles, characterized by a plateau in the shear elastic modulus (G') at low oscillation in dynamic rheological testing can significantly reduce the composites flammability. Hence, the effect of network formation of MWCNTs and MMT in epoxy resin is also studied to determine if rheological characterization can be used to predict the flammability of thermoset epoxy composites. The optical microstructure of MWCNTs and MMT suspensions in uncured epoxy resin were also studied to attempt to relate the state

* Corresponding author.
E-mail address: jwgilman@nist.gov (J.W. Gilman).
[1] Current address: Advance Composites Centre for Science and Innovation (ACCIS), Department of Aerospace Engineering, University of Bristol, UK.

0141-3910/$ – see front matter © 2010 Published by Elsevier Ltd.
doi:10.1016/j.polymdegradstab.2010.01.003

of dispersion of the particles to the rheological properties. The optical microstructure of MWCNTs and MMT suspension in uncured epoxy resin is discussed and is related to the rheological properties of the suspensions. The thermal degradation of epoxy/MMT and epoxy/MWCNTs composites was studied using TGA, whereas the flammability was studied using the National Institute of Standards and Technology (NIST) radiative gasification apparatus. Finally, a modeling study of the degradation of epoxy/MWCNTs and epoxy/MMT composites was studied to investigate the role of thermal conductivity changes, due to addition of nanoparticles, on mass loss rate (MLR) during gasification of epoxy composites.

2. Experimental and methods section

2.1. Materials and methods[2]

Bisphenol A based epoxy resin was purchased from Dow chemicals (DER 331). Amine based curing agent (Jeffamine D-400) was kindly provided by Huntsman Chemical Company. Highly aligned multiwall carbon nanotubes (Fig. 1) were grown from ferrocene/toluene solution at 760 °C by chemical vapor deposition method (CVD) at University of Cambridge [13]. Organo-modified montmorillonite (MMT) (Closite 30B) was kindly supplied from Southern Clay Products.

2.2. Dispersion and preparation of epoxy/MWCNT and epoxy/MMT composites

MWCNTs were dispersed in bisphenol A based epoxy resin at 25 °C using high shear mixing at 20 rads/s (200 rpm) for 2 h and the curing agent was mixed with epoxy/MWCNTs suspension. MMT was mixed with bisphenol A based epoxy resin at 80 °C for 2 h using high shear mixing at 200 rpm in order to achieve an intercalated clay structure after mixing. Epoxy/MWCNT with MWCNTs concentration 0.0003, 0.0025, 0.005 mass fraction and epoxy/MMT with MMT concentration of 0.021, 0.065 and 0.135 mass fraction were prepared. Samples were cured at 60 °C for 2 h and post-cured at 90 °C for 15 h. Circular disc shape samples (diameter 75 mm, 8 mm thick) of cured epoxy/MWCNTs and epoxy/MMT composites were prepared to test their flammability.

2.3. Characterization and measurements

The rheological measurements were carried out on the epoxy/MMT as well as epoxy/MWCNT samples immediately after mixing the curing agent using a TA instruments AR G2 rheometer (the variation in all the rheological measurements was less than ±5%). Wide angle X-ray diffraction (XRD) of epoxy/MMT nanocomposites was studied using Philips electronic instruments XRG 3100 using Cu $K_{\alpha 1}$ radiation ($\lambda = 0.154059$ nm) and step size of 0.048°. The flammability of cured epoxy/MWCNTs and neat epoxy samples was investigated in the NIST gasification apparatus by measuring the sample mass loss *vs*. time and recording the sample behavior using a video camera (Fig. 2) [14] (the variation in all the gasification apparatus measurements is less than ±10%). An external heat flux of 50 kW/m^2 and nitrogen atmosphere was used for the gasification apparatus. Thermal conductivity of cured epoxy and cured epoxy/MWCNTs composites was measured using a HotDisk TPS thermal analyzer with 9.7 mm radius Kapton sensor at 25 °C.

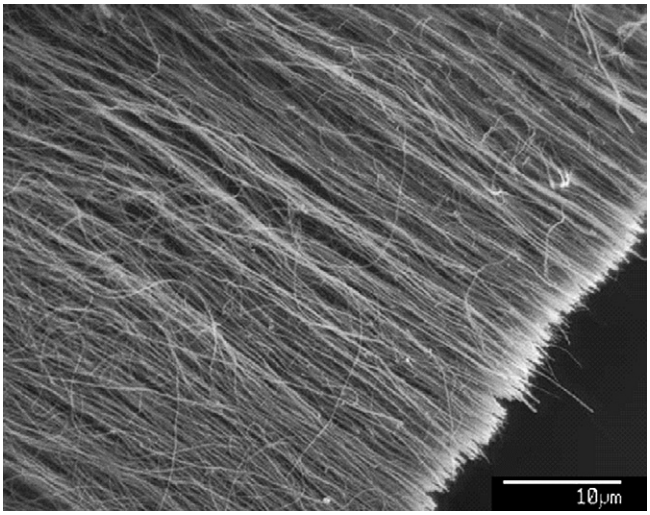

Fig. 1. Highly aligned chemical vapor deposition grown multiwall carbon nanotubes. The high alignment of MWCNTs allows them to easily exfoliate into individual MWCNTs dispersion using high shear mixing.

2.4. Modeling

The fire behavior of the nanocomposites was also investigated by making use of a model, Thermakin, that combines a continuum description of the transport of thermal energy within the solid (in a single dimension perpendicular to the sample surface) with Arrhenius kinetics for the decomposition of the polymer [15,16]. The overall behavior of a pyrolyzing object is described by mass and energy conservation equations. These equations are formulated in terms of rectangular finite elements. Each element is characterized by component masses and temperature. The model includes a description of the transport of gases through the condensed phase

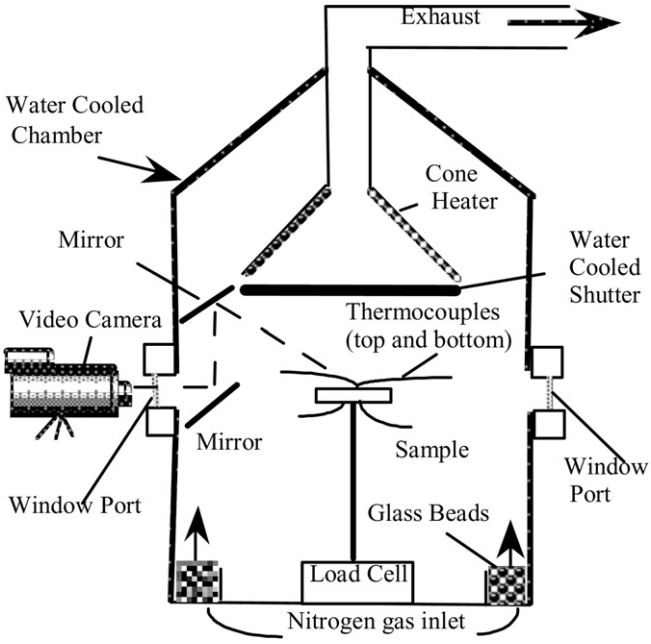

Fig. 2. Schematic of gasification apparatus.

[2] This work was carried out by the National Institute of Standards and Technology (NIST), an agency of the US government and by statute is not subject to copyright in USA. The identification of any commercial product or trade name does not imply endorsement or recommendation by NIST. The policy of NIST is to use metric units of measurement in all its publications, and to provide statements of uncertainty for all original measurements. In this document, however, data from organizations outside NIST are shown, which may include measurements in non-metric units or measurements without uncertainty statements.

Table 1
Model input.

Component	Density (kg/m^3)	Heat capacity ($J\,kg^{-1}\,K^{-1}$)	Thermal conductivity ($W\,K^{-1}\,M^{-1}$)	Gas transfer coefficient (m/s)	Absorption coefficient (m^{-1})	Emissivity
Epoxy	1140	$-1330 + 8.6\,T$	$0.2 + 4.7 \times 10^{-4}\,T$	10^{-5}	2.25	0.95
Epoxy Gas	1140	1000	0.4	10^{-5}	1.0	0.95
Epoxy Char	800	1000	1.0	10^{-5}	1.0	0.95
MMT	1300	1000	1.0	10^{-5}	5.00	0.95
Organic Treatment	1140	1000	0.4	10^{-5}	2.25	0.95
MWCNT	1300	1000	1.0	10^{-5}	100	0.95
MWCNT Char	1300	1000	100	10^{-5}	100	0.95
Air	11	1040	0.026	10^{-5}	0	0.75
Insulation	1000	1000	10^{-30}	10^{-30}	1000	0

and tracks changes in the volume of material. The complexity of the model can be altered by introducing or removing material components, which are characterized by temperature-dependent physical and chemical properties. Every component is characterized by density, heat capacity, thermal conductivity, gas transfer coefficient, emissivity, and absorption coefficient. The values used in our calculations are listed in Table 1. Components may undergo reactions. Each reaction may have one or two reactants and zero to two products. The rate of reaction is presumed to be proportional to the product of the reactant concentration(s) with rate constant $k(T) = A\exp(-Ea/RT)$, where A and Ea are the Arrhenius pre-exponential factor and activation energy and R is the gas constant.

The density of the epoxy resin was calculated from direct measurement of the mass and volume of the (circular) disk shaped samples used in the gasification experiments. The decomposition of the epoxy was described as a single step, first order reaction resulting in the formation of both gas and carbonaceous char. The kinetic parameters ($Ea = 260$ kJ/mol and $A = 8.7 \times 10^{17}\,s^{-1}$) governing the rate of this reaction and the char yield (6% by mass) were obtained from thermogravimetric analysis (TGA). All other values, including the enthalpy of decomposition (340 kJ/kg), optical properties (absorption coefficients and emissivities), heat capacities, and the thermal conductivities of the epoxy resin and char were estimated by fitting the predicted mass loss rate (MLR) curves to the experimental measurements. Note that the thermal conductivity and heat capacity were represented by linear functions of the temperature (in Kelvin), which was necessary to capture the qualitative features of the epoxy MLR curve. Although past experience has indicated that it is not always possible to obtain meaningful solutions by fitting MLR curves, previous measurements made on similar materials by the developers of Thermakin [17–21] facilitated our ability to choose realistic values for these properties.

The nanoadditives were treated as solid objects that absorb and emit radiation without decomposing. Values for the thermal conductivities of the MMT and MWCNT nanoadditives were estimated by requiring that the volume averaged thermal conductivities were consistent with experimental measurements on the corresponding nanocomposites (see Fig. 8). Other values for the thermo physical and optical properties (see Table 1) were obtained by fitting the calculated MLR curves to the results of the gasification experiments; as described in the preceding paragraph. As the surrounding polymer decomposes, the nanoadditives are envisioned to become part of a continuous network that occupies a fraction of the volume of the original sample. This process was represented by a single step, first order reaction with zero enthalpy and kinetic parameters identical to those used for the decomposition of the epoxy. The fraction of the sample volume occupied by the nanoadditive network was determined by varying its density until the predicted values for the peak MLRs (PMLRs) were consistent with the experimental observations. The TGA data in Fig. 11 clearly indicate that, although the onset of decomposition was not affected by the presence of the MWCNTs, it occurred at lower temperatures as the loading of MMT was increased. While the source of this behavior is not clear, we found that the inclusion of an additional reaction corresponding to the decomposition of the low molecular weight organic surfactant improved agreement between the calculated and experimental MLR curves, particularly early on in the degradation process. The values of the reaction enthalpy, activation energy, and pre-exponential factor used to describe the thermodynamics and kinetics of this reaction were 100 kJ/kg, 200 kJ/mol and $8.7 \times 10^{13}\,s^{-1}$, respectively.

3. Results

Fig. 3 shows the optical microstructure of epoxy/MWCNTs composites at room temperature right after mixing it with Jeffamine and before starting the curing process. Optical microstructure of the MWCNTs shows loosely packed isolated aggregates of the MWCNTs at 0.00035 mass fraction of MWCNTs in epoxy. Even though highly aligned MWCNTs were used (which are much easier to disperse as compared to commercial MWCNTs), the MWCNTs show weak aggregation, due to unfavorable interaction with the epoxy matrix. Such morphology of weak aggregation of MWCNTs was reported previously [22–24]. With increase in MWCNT concentration, the aggregate size increases and eventually forms an interconnected network of MWCNTs in epoxy, as seen in microstructure of 0.0025 mass fraction and 0.005 mass fraction of MWCNTs in epoxy. Similar microstructure of weakly aggregated MWCNTs was reported previously by Rahatekar et al. [22], Martin et al. [23] and Hobbie et al. [24]. Weakly aggregated MWCNTs microstructure was reported to be very effective in achieving rheological and electrical percolation at very low volume fractions of MWCNTs [22–25].

Fig. 4 shows XRD data for epoxy/MMT composites. The d-spacing from the XRD data for MMT is found to be ≈ 3.48 nm which confirms that the MMT in the epoxy has an intercalated structure. Although the length of the MMT platelets dispersed in epoxy is about 200 nm [12], the optical microstructure shows a much larger particle size than 200 nm. The MMT tactoid aggregates form approximately 5 to 10 μm mesoscale structures. Such a microstructure in polymer laponite clay has also been reported by Loizou et al. [26]. With increase in the mass fraction of MMT, the aggregates become larger and eventually span to form a well-connected network (0.135 mass fraction MMT/epoxy sample).

The rheological properties of MMT/epoxy and epoxy/MWCNTs composites were also measured. Rheological characterization of nanoclay or MWCNTs has been used to detect network formation of nanoparticles in suspension which has been shown to reduce the flammability of PMMA/nanoparticle composites [2]. Hence, a similar study is conducted here. Fig. 5 shows elastic shear modulus (G') measurements of epoxy/MMT composites immediately after mixing with Jeffamine curing agent (before the composites is cured) as a function frequency of oscillation of the rheometer plate. As seen

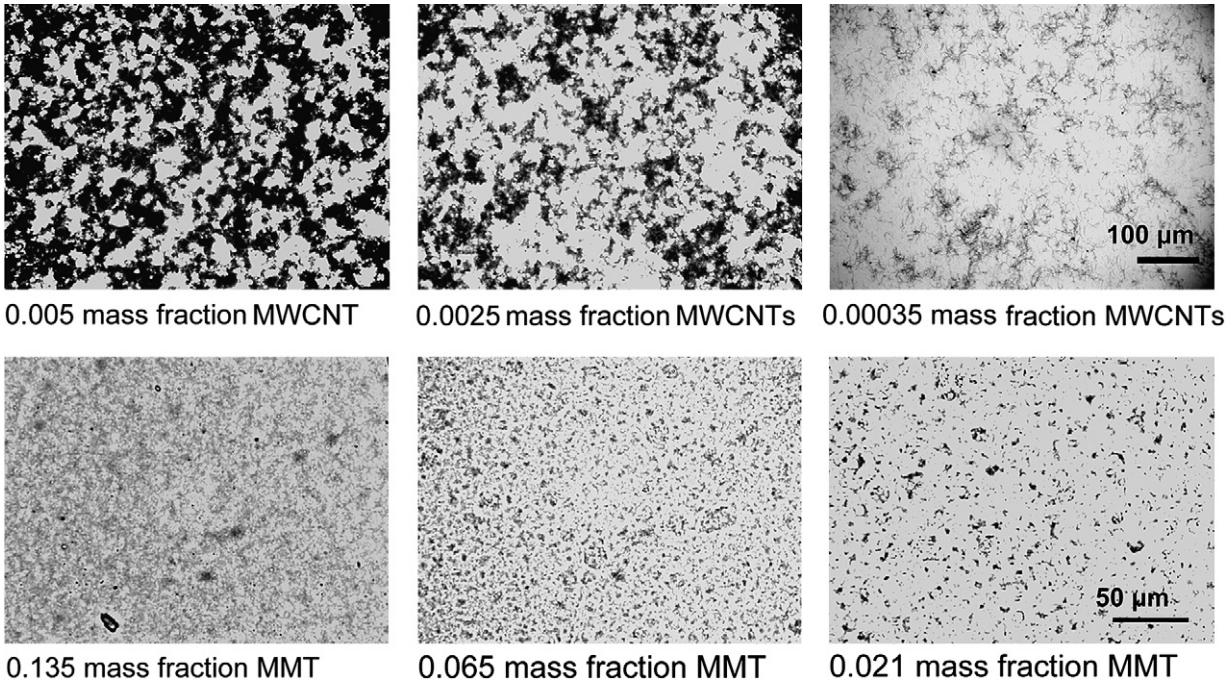

Fig. 3. Optical microstructure of epoxy/MWCNTs and epoxy/MMT composites. Both MMT and MWCNT suspension in epoxy show aggregates which eventually form interconnected network with increase in concentration.

in Fig. 5 the 0.135 mass fraction epoxy/MMT shear elastic modulus G' dominates over the viscous modulus G'' at low frequency of oscillation (ω), this is a characteristic of solid-like behavior due to network formation of nanoparticles in the suspension. In 0.065 mass fraction and 0.021 mass fraction epoxy/MMT nanocomposite samples G'' dominates G' over the entire range of oscillation frequency, which confirms that these samples behave liquid-like and hence do not form a network of MMT in the epoxy. The optical microstructure observed for epoxy/MMT suspensions also indicate isolated aggregates of MMT tactoids for 0.065 mass fraction and 0.021 mass fraction MMT and a continuous network of MMT aggregates for the 0.135 mass fraction sample which is consistent with the rheological data.

Rheological measurements of G' of MWCNT/epoxy suspensions show a similar trend (network formation of MWCNTs in epoxy) to that of MMT/epoxy suspension, but with a much lower percolation threshold (Fig. 6). For the 0.0003 mass fraction epoxy/MWCNTs sample G'' dominates over G' the entire frequency range which indicates that the MWCNTs do not form a network at this concentration. Hence for 0.0025 mass fraction and 0.005 mass fraction epoxy/MWCNTs samples G' is almost constant at low frequency of oscillation and G' dominates over G'' for both of these samples over a wide range of oscillation frequency. This is a signature of solid-like behavior due to network formation of MWCNTs in epoxy resin. The optical microstructure of the 0.0025 mass fraction and 0.005 mass fraction epoxy/MWCNT (Fig. 3) sample also shows a good interconnected network of MWCNT aggregates which is consistent with the rheological data. The nanoparticle network is formed in epoxy/MWCNTs above 0.0003 mass fraction of MWCNTs whereas in epoxy/MMT suspension the network forms only above 0.065 mass fraction of MMT. This large difference in critical concentration for network formation is most likely because MWCNTs have a significantly higher aspect ratio (≈625) than MMT and also because of

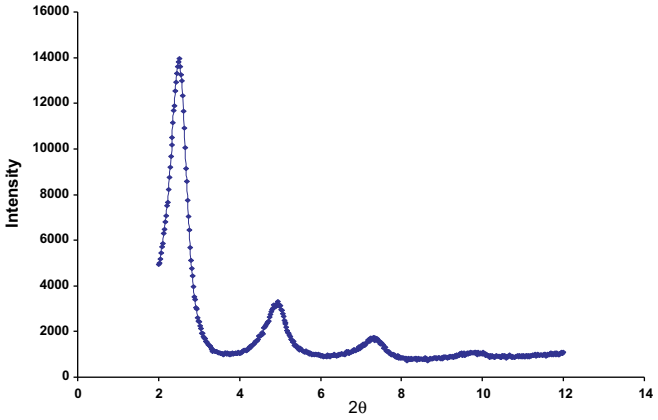

Fig. 4. X-ray diffraction of epoxy/MMT nanocomposites showing in the D-spacing ≈3.48 nm of MMT tactoids.

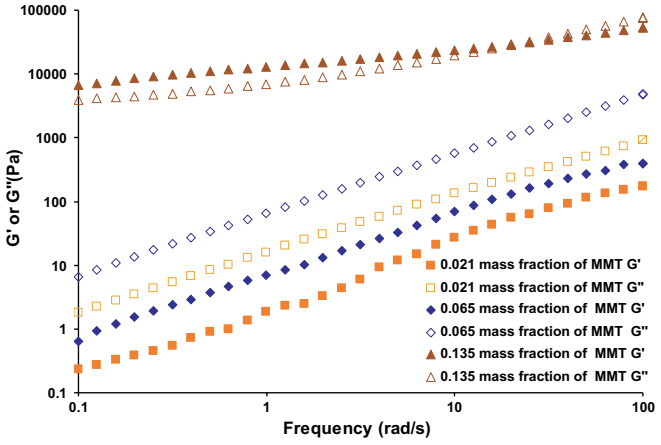

Fig. 5. Oscillatory shear test for epoxy/MMT samples. The 0.135 mass fraction MMT/epoxy sample show that G' independent at low oscillation frequency which is characteristic of network formation of MMT in epoxy resin.

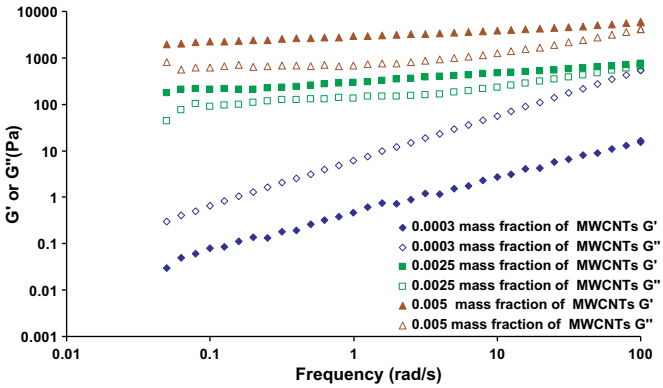

Fig. 6. Oscillatory shear test for epoxy/MMWCNTs samples. 0.005 mass fraction and 0.0025 mass fraction epoxy/MWCNTs sample show that G′ is independent of low oscillation frequency which is characteristic of network formation of MWCNTs in epoxy resin.

high alignment of CVD grown MWCNTs, which can be completely exfoliate into individual MWCNTs (debundled) as compared to MMT platelets, which in the samples are intercalated but not completely exfoliated.

The flammability of samples are evaluated using the gasification apparatus (Fig. 5) which measures the MLR of the sample due to exposure to a constant heat flux under an inert atmosphere. There are three unique features of the gasification apparatus used for flammability testing. First, the gasification apparatus allows us to study the condensed phase during pyrolysis in the absence of oxidation, since the gasification is carried out in a nitrogen atmosphere. Secondly, the total heat flux which the samples are exposed to remains nearly constant from sample to sample, as there is no heat feedback from combustion in the gas phase, and lastly, one can make optical (video) observations of the thermal degradation process due to absence of interference from flame. Details of the gasification apparatus are disused in a previous publication [14].

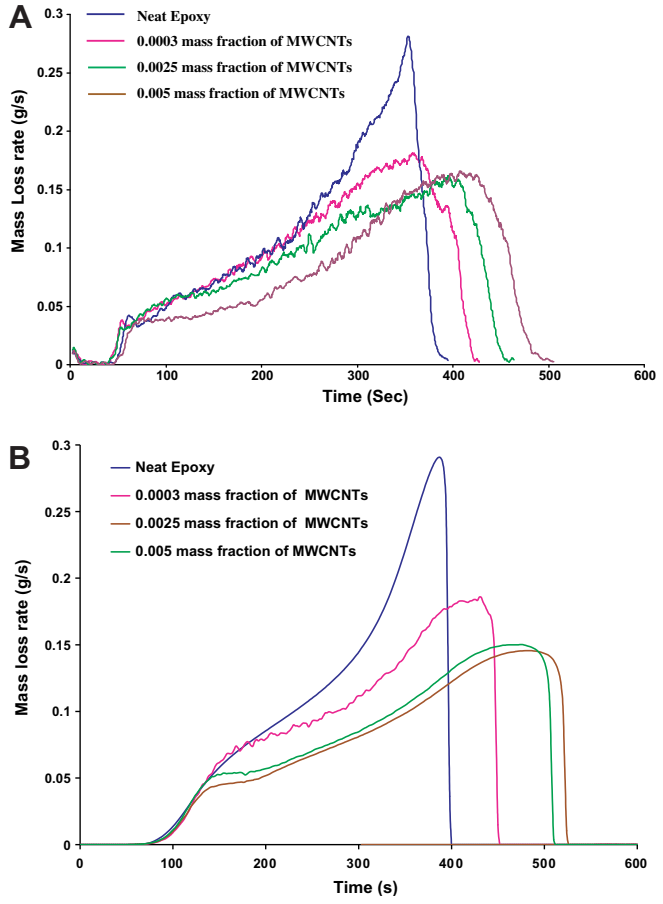

Fig. 7. [A] Experimental data of mass loss rate for epoxy/MWCNTs composites. [B] Modeling data of mass loss rate of epoxy MWCNTs composites.

Table 2
Results of modeling.

Nanoadditive	Loading (mass fraction)	Network thickness (m)	Network density (kg/m^3)	Thermal conductivity[a] ($W K^{-1} M^{-1}$)	PMLR (g/s)
None	0.0	0.0	0.0	0.341	0.29
MMT	0.021	1.0×10^{-3}	270	0.349	0.26
MMT	0.065	2.3×10^{-3}	190	0.367	0.19
MMT	0.135	6.5×10^{-3}	115	0.395	0.13
MWCNT	0.0003	2.1×10^{-3}	2.0	0.355	0.19
MWCNT	0.0025	3.8×10^{-3}	7.5	0.451	0.16
MWCNT	0.005	5.0×10^{-3}	10.8	0.560	0.16

[a] At 300 K.

MLR for epoxy/MWCNT composites are shown in Fig. 7A. Reduction in peak of mass/heat release rate is an important factor in controlling flame spread [27]. For the 0.005 mass fraction sample as well as the 0.0025 mass fraction MWCNTs/epoxy sample the reduction in the peak MLR was observed to be almost 50% of the value obtained for neat epoxy. The 0.0003 mass fraction MWCNT sample shows ≈40% reduction in the peak MLR as compared to peak MLR of epoxy. There is also significant delay in the total time required for complete mass loss for all epoxy/MWCNT samples which increased with increase in the mass fraction of MWCNTs in epoxy. Hence, reduction in the MLR during gasification is an important feature in epoxy/MWCNTs composites.

Modeling provided additional insights into the effect of the nanoadditives on the MLRs of the nanocomposites. In order to have a better understanding of the mechanism of MLR during gasification we carried out modeling of the gasification of neat epoxy, MMT/epoxy and MWCNTs/epoxy samples. The results of the modeling of MWCNTs/epoxy and neat epoxy gasification are shown in Fig. 7B and summarized in Table 2. Although there are some minor discrepancies between the calculated and experimental MLR curves, the overall agreement is reasonably good, which instills

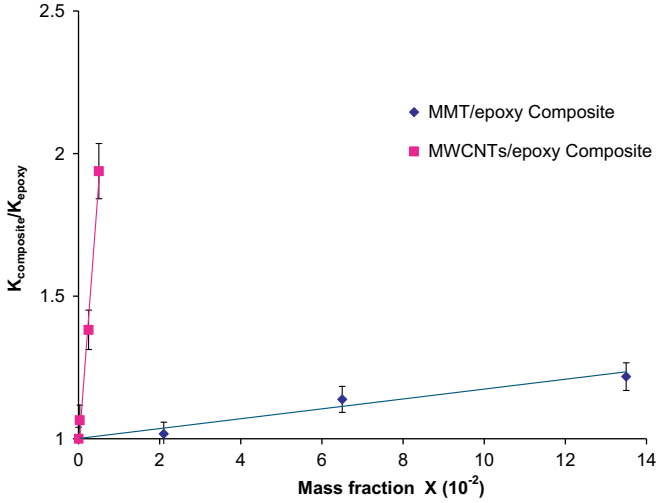

Fig. 8. Relative thermal conductivity of epoxy/MWCNTs shows about 2-fold increase in thermal conductivity of 0.005 mass fraction epoxy/MWCNTs samples as compared to the thermal conductivity of neat epoxy. MMT/epoxy samples, which show significantly less increase in thermal conductivity.

some confidence in the validity of conclusions drawn from these calculations. They indicate that the primary mechanism by which these nanoadditives effect a reduction in MLR is re-radiation of the thermal energy incident on the sample surface. More specifically, once the surrounding polymer is gasified, the nanoadditives form a protective layer on the surface of the sample [2]. As the temperature of the nanoadditive layer rises, it emits radiation in proportion to the fourth power of its temperature in accordance with the Stefan–Boltzmann equation. As a consequence, the thermal energy reaching the underlying polymer is reduced (thereby resulting in a lower MLR); effectively becoming zero when the network comes into thermal equilibrium with the source of radiant energy at a temperature of about 960 K.

The effectiveness of re-radiation in reducing the MLR depends on the volume (or, equivalently, the thickness of the protective layer formed by the nanoadditives) and the thermal conductivity of the nanoadditive network. All other things being equal, the peak MLR decreases as the thickness of this protective layer increases and as its thermal conductivity decreases. The MWCNTs have large aspect ratios, which may enable them to form a strong protective layer at very low densities. However, the effectiveness of the MWCNT network in shielding the underlying polymer is eventually undermined because thermal conductivity increases with MWCNT loading. At high loadings (or, equivalently, high thermal conductivities), the thickness of the protective layer becomes insufficient during the later stages of the thermal decomposition of the sample and the underlying polymer heats up, resulting in an increase in PMLR. The break-even point appears to occur for MWCNT loadings in the vicinity of 0.005 mass fraction, Fig. 8 shows the relative change in thermal conductivity with increase in the MWCNT mass fraction as compares to thermal conductivity of neat cured epoxy matrix at 25 °C. As seen from Fig. 8, the thermal conductivity for 0.005 mass fraction epoxy/MWCNTs is significantly higher than 0.0025 mass fraction epoxy/MWCNT composite. It is very difficult to measure the thermal conductivity of epoxy/MWCNTs at the gasification temperature, most likely it is going to be higher that thermal conductivity at room temperature. This is because epoxy resin, which has poor thermal conductivity, degrades and gasifies during the experiment which will further increase the effective concentration of MWCNT in the protective surface layer. Due to higher thermal conductivity of epoxy/MWCNTs, the heat transfer to the degrading polymer molten layer below the charring layer will increase, hence we observe a slight increase in the peak of mass release rate for 0.005 mass fraction epoxy/MWCNTs sample, which

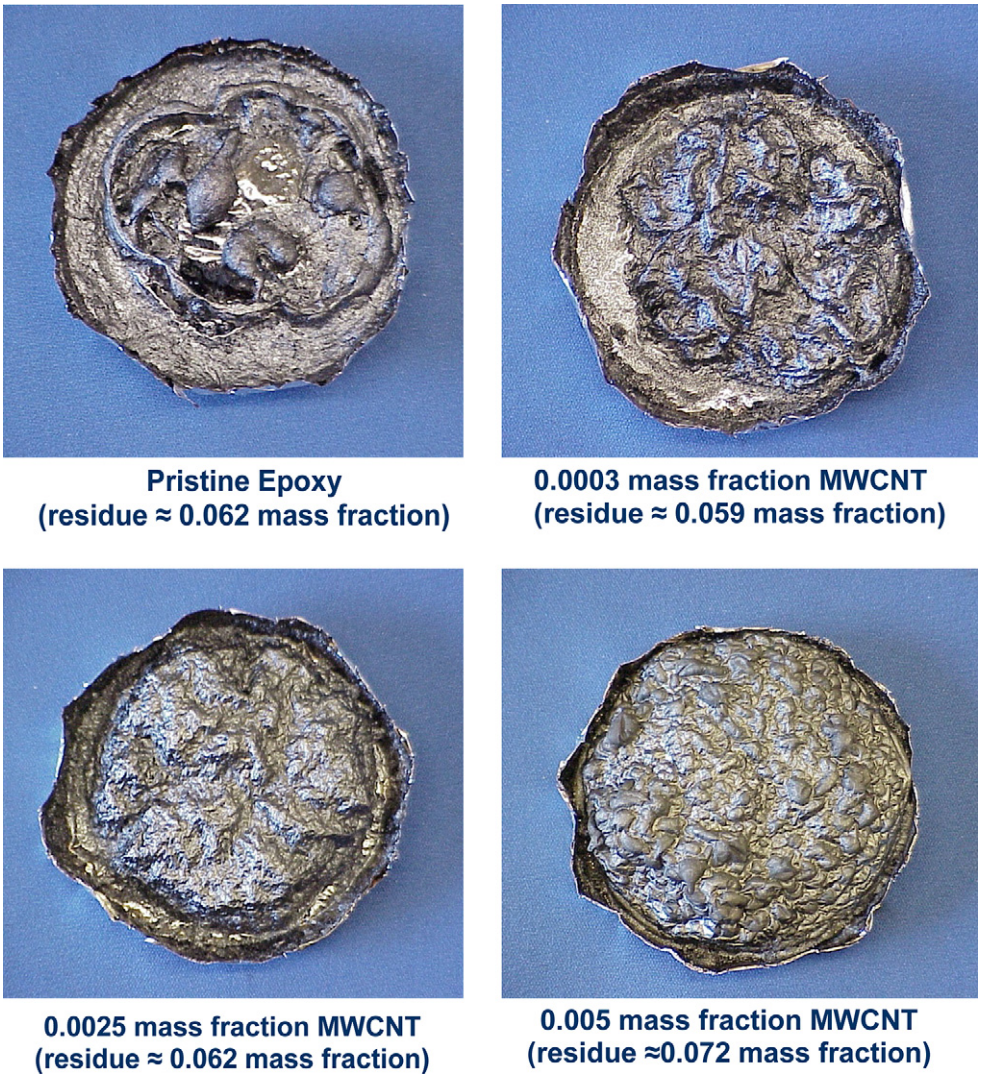

Fig. 9. Residue for epoxy/MWCNTs samples after gasification test. 0.5 mass fraction and 0.25 mass fraction epoxy/MWCNT samples show good residue integrity as compared to neat epoxy and 0.035 mass fraction epoxy/MWCNT samples. Unlike epoxy/MMT residue, epoxy/MWCNTs samples residue do not show any visible surface cracks.

is consistent with our experimental data as well as modeling predictions (Fig. 7). Similar reversal of the trend in the peak mass loss rate (PMLR) with increase in MWCNTs mass fraction is also reported by Kashiwagi et al. [8].

The residue formed after gasification for 0.0003 mass fraction MWCNT/epoxy sample shows good residue integrity, i.e., the residue retains the original shape of the sample. No visible surface cracks (Fig. 9) are observed which helps to reduce the mass loss from the surface during gasification. Better residue integrity may help explain the delay in the total time required for complete mass loss for 0.0003 mass fraction epoxy/MWCNT. The PMLR reduction improves further to 45% for 0.0025 mass fraction MWCNTs/epoxy samples. Improvement in the residue integrity (Fig. 9) as well as further increase in total time required for complete mass loss is observed (Fig. 7). With further addition of MWCNTs (0.005 mass fraction MWCNTs), the peak of MLR increase slightly compared to 0.0025 mass fraction MWCNT/epoxy composites. However, for 0.005 mass fraction MWCNT composites, the initial MLR profile is lot lower than the rest of the samples (Fig. 7A). Hence, we believe that even if the peak of MLR for 0.005 mass fraction MWCNTs sample is slightly higher than that for 0.0025 mass fraction MWCNT/epoxy, the significantly lower initial mass loss of 0.005 mass fraction MWCNT/epoxy sample represents an overall improvement in flammability. MWCNTs have very high thermal conductivity. The presence of MWCNTs in epoxy reduces the mass loss of the volatiles at the surface of epoxy/MWCNT, but with increase in amount of MWCNT the thermal conductivity of the epoxy MWCNTs increases. The increase in the thermal conductivity of 0.135 mass fraction MMT/epoxy sample is significantly less (about 20% increase relative to the neat epoxy) as compared to MWCNT/epoxy samples (Fig. 8).

The residue integrity for 0.0025 mass fraction and 0.005 mass fraction epoxy/MWCNTs appears to be better than that for 0.0003 mass fraction epoxy/MWCNTs and neat epoxy samples (Fig. 9). The residue yield of all MWCNTs/epoxy samples is not significantly different than the residue yield of pure epoxy sample. However, there is clear improvement in residue integrity and reduction in peak MLR, initial MLR and time required for complete mass loss for all the MWCNT/epoxy samples when compared with pure epoxy samples.

Fig. 10A shows the MLR as a function of time for neat epoxy and epoxy/MMT composites from gasification experiments. As seen in Fig. 10A, there is about 50% reduction in PMLR as well as a significant delay in the complete mass loss for the 0.135 mass fraction epoxy/MMT composites as compared to neat epoxy sample. There is also a 30% decrease in the peak of MLR at a clay concentration of 0.065 mass fraction and a 10% reduction in peak of MLR for 0.023 mass fraction MMT/epoxy composite. Fig. 10B shows the modeling results of the gasification of the neat epoxy and MMT/epoxy samples. There is good agreement with the mass loss rate curves obtained experimentally. It is of interest to note that the early increase in the MLR of the MMT/epoxy composites as compared to neat epoxy is reproduced in the model calculations. This behavior was not evident in the TGA (Fig. 11B) or MLR curves obtained from the MWCNTs/epoxy samples. In fact, quite to the contrary, the MWCNT/epoxy samples exhibit a distinct reduction in MLR with

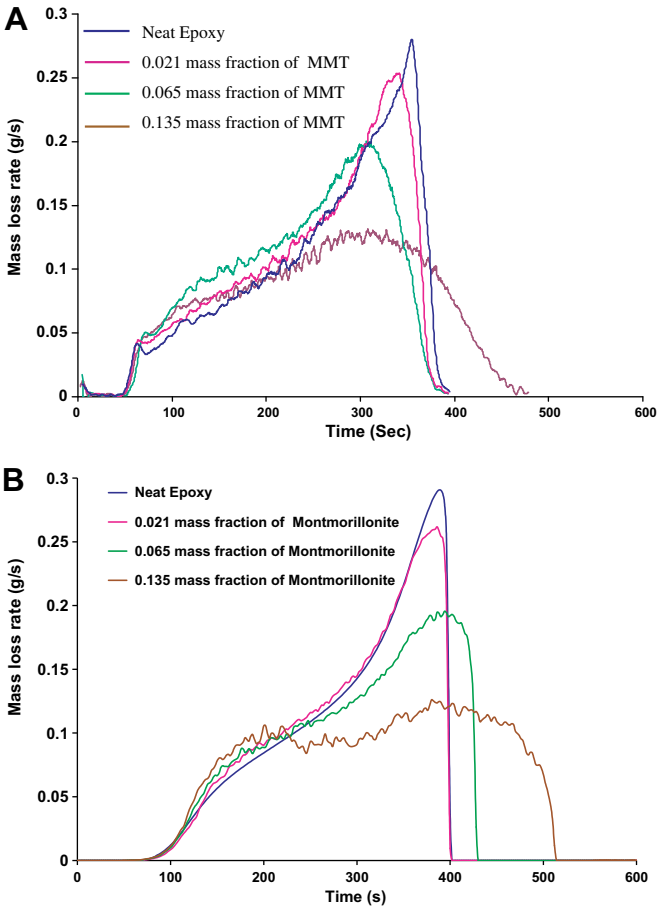

Fig. 10. [A] Experimental data of mass loss rate for epoxy/MMT composites. [B] Modeling data of mass loss rate of epoxy/MMT composites.

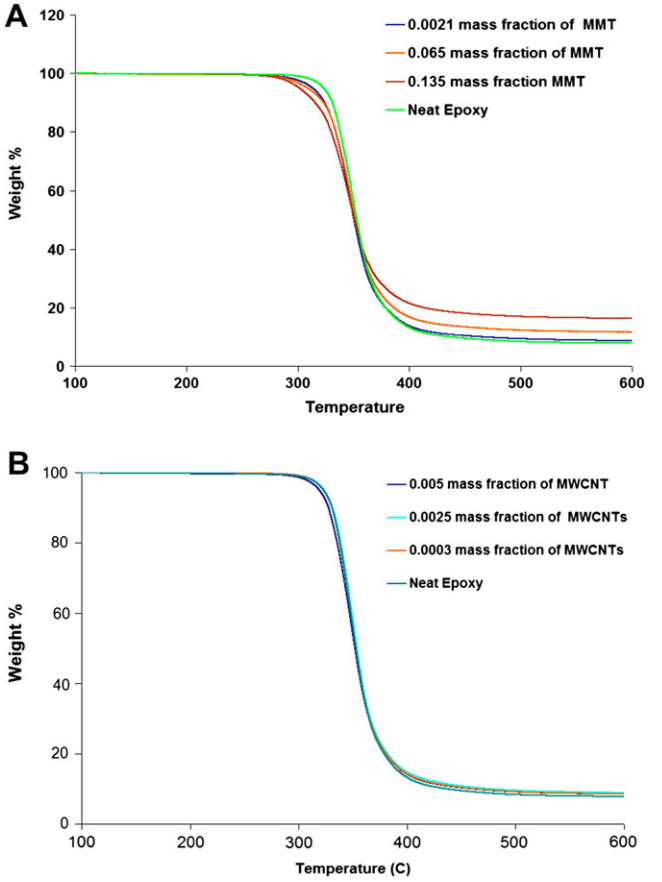

Fig. 11. Thermogravimetric data of decomposition of [A] epoxy and epoxy/MMT composites showing early decomposition of epoxy/MMT composites with increase in mass fraction of MMT. [B] Epoxy and epoxy/MWCNT composites which shows practically no change in the decomposition of epoxy/MMT composites as compared to neat epoxy.

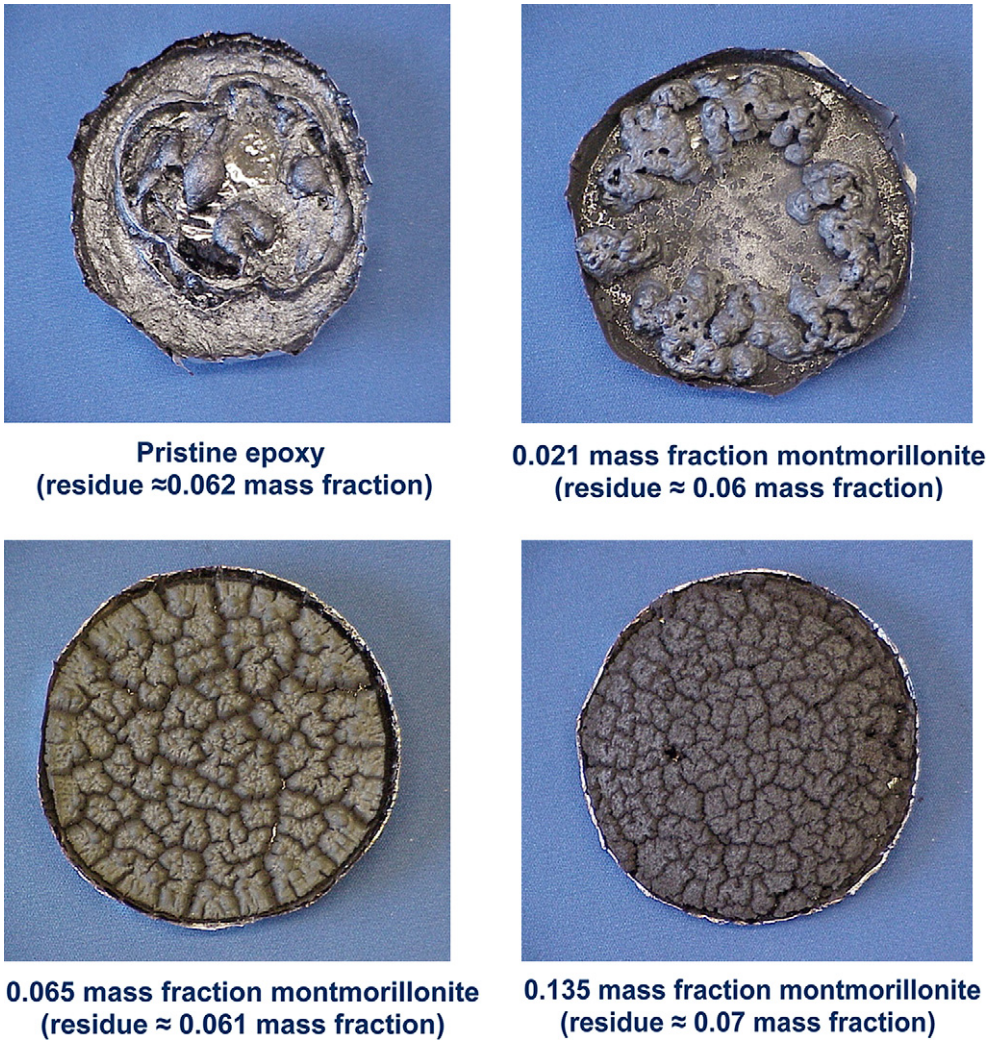

Fig. 12. Residue for epoxy/MMT samples after gasification test. 0.135 mass fraction and 0.065 mass fraction epoxy/MMT samples show good integrity as compared to neat epoxy and 0.021 mass fraction epoxy/MMT samples. However large surface cracks are visible on the 0.135 mass fraction and 0.065 mass fraction epoxy/MMT samples. The residue is calculated after subtraction of the inorganic residue left over from MMT.

increasing loading of MWCNTs, which is also reproduced in the model calculations (Fig. 7).

Fig. 12 shows the residue after gasification experiments of epoxy and epoxy/MMT composites. The residue after the gasification experiment for 0.135 mass fraction and 0.065 mass fraction epoxy/MMT show good integrity (no visible surface cracks). Neat epoxy produces a small amount of residue, however the residue integrity of pure epoxy sample does not seem to be good. The 0.021 mass fraction epoxy/MMT sample shows poor residue integrity as well, however, a small reduction (10%) was seen in the peak of MLR for this sample. Residue integrity is an important feature from the point of view of dripping of polymers during combustion. Dripping of polymers during combustion can increase flame spread rate, however the good residue integrity seen in 0.135 mass fraction and 0.065 mass fraction epoxy/MMT samples is likely to avoid dripping during combustion. Even though the residue integrity of 0.065 and 0.135 mass fraction samples is good, these samples show large visible surface cracks in the residue. The formation of cracks on the surface of the pyrolyzing polymer during gasification allows the thermal energy to penetrate deep into the underlying polymer affecting the efficiency of the thermal barrier generated by the nanoadditive. The residue will work effectively as a protective barrier, if there is a continuous protective layer of nanoparticle and residue formed on the surface of the sample. The residue for all the MWCNTs/epoxy samples i.e. 0.0003 mass fraction, 0.0025 mass fraction, and 0.005 mass fraction Epoxy/MWCNTs samples do not show visible surface cracks, which were clearly seen in the residue of epoxy/MMT samples. The high aspect ratio of MWCNTs most likely acts as reinforcement in the residue and do not allow the residue to crack on the surface. The better residue integrity of epoxy/MWCNTs samples may be the reason for the delay in complete mass loss as compared to epoxy/MMT samples.

The 0.135 mass fraction epoxy/MMT sample shows a 50% decrease in PMLR as well as a significant delay in the complete mass loss as compared to rest of the samples (Fig. 10A). The 0.065 mass fraction epoxy/MMT samples also show 20% reduction in peak MLR and good residue integrity after gasification. However, rheological data (G') does not show network formation for 0.065 mass fraction MMT/epoxy sample. The neat epoxy sample forms residue after gasification which was not seen in a previous study of PMMA/nanoparticle composites. We believe that the residue formation of epoxy reduces absolute need for network formation of nanoparticles, hence, even when MMT does not form a solid-like network at 0.065 mass fraction, it still is able to reduce the peak of mass loss

during gasification. Thus, in this case, rheological measurements do not strictly correlate to flammability data like previously observed for thermoplastic non-charring polymers [2].

For epoxy/MWCNTs as well as epoxy/MMT, we could not establish a good correspondence between the rheological properties (network formation of nanoparticles) and the reduction in the peak of MLR or the residue integrity of the samples. 0.0025 mass fraction and 0.005 mass fraction epoxy/MWCNTs samples show a network formation of MWCNTs which is determined using G' measurement. 0.0003 mass fraction MWCNTs/epoxy sample does not show network formation of MWCNTs based on measurement of G' yet there is significant reduction in peak MLR. Once again, for thermoset epoxy/nanoparticle composites, there is not necessarily a direct correlation between flammability and rheolological properties for epoxy resin. Residue (char) from epoxy (which was not seen for PPMA/MWCNTs composites in a previous study [4]) and MWCNTs may be able to form an effective protective layer which reduces the MLR, which may effectively form a barrier reducing peak MLR even when MWCNTs by themselves do not form a network. There is also an additional factor of thermal conductivity which plays an important role in determining the peak of MLR besides the effect protective layer formation of MWCNTs. Hence, for MWCNTs more than 0.005 mass fraction in epoxy matrix will result in higher PMLR even if there is network formation of MWCNTs.

4. Conclusions

This work was focused on comparing the flammability of epoxy/MWCNT and epoxy/MMT composites. Both epoxy/MWCNTs and epoxy/MMT nanocomposites showed significant reduction in the PMLR during gasification experiments. The PMLR for 0.005 mass fraction and 0.0025 mass fraction epoxy/MWCNTs composites was reduced by 45% as compared to neat epoxy. In this study, we were able to achieve 45% decrease in PMLR at very small amount (0.0025mass fraction) MWCNTs, much smaller than reported previously with either using MWCNTs (0.02 mass fraction) [8] or SWCNTs (0.005 mass fraction) [5] composites. We attribute this effect to highly aligned MWCNTs which can be easily exfoliated (debundle) using high shear mixing. The 0.135 mass fraction of MMT was required to observe a similar reduction in PMLR for epoxy/MMT composites as compared to 0.0025 mass fraction of MWCNTs. Both MWCNTs and MMT composites seem to show improved residue integrity (above a concentration to form nanoparticle network) as compared to neat epoxy. However, visible surface cracks were seen on the surface of epoxy/MMT residue indicating that the residue strength of epoxy/MWCNTs may be better than that for the epoxy/MMT. Peak of MLR decreases by 45% when MWCNTs form a network in epoxy. For 0.005 mass fraction MWCNTs there was slight increase in the peak of MLR, however, this sample showed a significantly less mass loss as compared to the rest of the samples during initial part of gasification experiment. For thermoset epoxy, unlike PMMA, residue from neat crosslinked epoxy resin is obtained in gasification experiments. The effect of residue formation from neat epoxy appeared to have reduced the absolute necessity of network formation of nanoparticles in order to reduce the peak MLR and improvement in the residue integrity of the samples. Thus, even if 0.0003 mass fraction MWCNTs/epoxy sample and 0.065 mass fraction MMT/epoxy sample shows no rheological network formation, these samples still are able to reduce the PMLR during gasification.

Modeling of gasification of MWCNT/epoxy and MMT/epoxy nanocomposites resulted in good fits to the experimental mass loss rate curves. Since the nanoadditives were treated in the model as inert objects that can only absorb and emit radiation, the good agreement between the model calculations and experimental measurements is taken as evidence that re-radiation of the absorbed heat is the primary mechanism by which these nanoadditives effect a reduction in MLR. The effectiveness of re-radiation in reducing the MLR depends on the volume (or, equivalently, the thickness of the protective layer formed by the nanoadditives) and the thermal conductivity of the nanoadditive network. All other things being equal, the peak MLR decreases as the thickness of this protective layer increases and as its thermal conductivity decreases. The MWCNTs are more effective than MMT at low loadings because of their rope or fiber like structure, which enables them to form strong networks at very low densities. However, the effectiveness of the MWCNT network in shielding the underlying polymer is eventually undermined because its thermal conductivity increases with MWCNT loading. At high loadings (or, equivalently, high thermal conductivities), the thickness of the protective layer becomes insufficient and the underlying polymer heats up during the later stages of the thermal decomposition process resulting in an increase in PMLR. The break-even point appears to occur for MWCNT loadings in the vicinity of 0.5 wt%. Since MMT has much lower thermal conductivity than MWCNTs, this point is never attained for the MMT nanocomposites. The efficacy of increasing the loading of MMT is, however, limited by its poor miscibility in the polymer.

References

[1] Gilman JW, Jackson CL, Morgan AB, Harris R, Manias E, Giannelis EP, et al. Flammability properties of polymer-layered-silicate nanocomposites, polypropylene and polystyrene nanocomposites. Chem Mater 2000;12(7):1866–73.
[2] Kashiwagi T, Du FM, Douglas JF, Winey KI, Harris RH, Shields JR. Nanoparticle networks reduce the flammability of polymer nanocomposites. Nat Mater 2005;4:928–33.
[3] Beyer G. Carbon nanotubes as flame retardants for polymers. Fire Mater 2002;26(6):291–3.
[4] Kashiwagi T, Harris Jr RH, Zhang X, Briber RM, Cipriano BH, Raghavan SR, et al. Flame retardant mechanism of polyamide 6 – clay nanocomposites. Polymer 2004;45(3):881–91.
[5] Kashiwagi T, Du F, Winey KI, Groth KM, Shields JR, Bellayer SP, et al. Properties of polymer nanocomposites with single-walled carbon nanotubes: effects of nanotube dispersion and concentration. Polymer 2005;46(2):471–81.
[6] Kashiwagi T, Grulke E, Hilding J, Groth KM, Harris Jr RH, Butler KM, et al. Thermal and flammability properties of polypropylene/carbon nanotube nanocomposites. Polymer 2004;45(12):4227–39.
[7] Cipiriano BH, Kashiwagi T, Raghavan SR, Yang Y, Grulke EA, Yamamoto K, et al. Effects of aspect ratio of MWNT on the flammability properties of polymer nanocomposites. Polymer 2007;48(20):6086–96.
[8] Schartel B, Potschke P, Knoll U, Abdel-Goad M. Fire behaviour of polyamide 6/multiwall carbon nanotube nanocomposites. Eur Polym J 2005;41(5):1061–70.
[9] Schartel B, Braun U, Knoll U, Bartholmai M, Goering H, Neubert D, et al. Mechanical, thermal, and fire behavior of bisphenol a polycarbonate/multiwall carbon nanotube nanocomposites. Polym Eng Sci 2008;48(1):149–58.
[10] Bocchini S, Frache A, Camino G, Claes M. Polyethylene thermal oxidative stabilization in carbon nanotubes based nanocomposites. Eur Polym J 2007;43(8):3222–35.
[11] Tidjani A, Wilkie CA. Photo-oxidation of polymeric-inorganic nanocomposites: chemical, thermal stability and fire retardancy investigations. Polym Degrad Stab 2001;74(1):33–7.
[12] Gilman JW, Kashiwagi T, Nyden MR, Brown JET, Jackson CL, Lomakin SM, et al. Chemistry and technology of polymer additives. Blackwell Science Inc; 1999.
[13] Singh C, Shaffer MSP, Koziol KKK, Kinloch IA, Windle AH. Towards the production of large-scale aligned carbon nanotubes. Chem Phys Letts 2003;372(5–6):860–5.
[14] Austin PJ, Buch RR, Kashiwagi T. Gasification of silicone fluids under external thermal radiation. Part I. Gasification rate and global heat of gasification. Fire Mater 1998;22(6):221–37.
[15] Stoliarov SI, Lyon RE. Thermo-kinetic model of burning. Federal aviation administration technical note; DOT/FAA/AR-TN08/17; May 2008.
[16] Stoliarov SI, Lyon RE. Thermo-kinetic model of burning for pyrolyzing materials. Fire Safety Science – Proceedings of the ninth international symposium (International Association for Fire Safety Science), in press.
[17] Stoliarov SI, Crowley S, Lyon RE, Linteris GT. Prediction of the burning rates of non-charring polymers. Combustion and Flame 2009;156:1068–83.
[18] Stoliarov S, Lyon R. Thermo-kinetic model of burning for pyrolyzing materials. Fire Safety Science 2009;9:1141–52.
[19] Stoliarov SI, Crowley S, Lyon RE, Linteris GT. Prediction of the burning rates of non-charring polymers. Combustion and Flame 2009;156:1068–83. Elsevier.

[20] Nyden MR, Stoliarov SI, Ganesan V, Khounlavong L. Modeling the dispersion and agglomeration of carbon nanotubes in polymers. ACS PMSE Preprints; 2008.
[21] Nyden MR, Stoliarov SI, Ganesan V, Khounlavong L. Modeling the dispersion and agglomeration of carbon nanotubes in polymers. In: 19th BCC Conf. On Flame Retard., Stamford, CT; 2007.
[22] Rahatekar SS, Koziol KK, Butler S, Elliott JA, Shaffer MSP, Mackley MR, et al. Optical Microstructure and viscosity enhancement for an epoxy resin matrix containing multiwall carbon nanotubes. J Rheol 2006;50(5):599–610.
[23] Martin CA, Sandler JKW, Shaffer MSP, Schwarz MK, Bauhofer W, Schulte K, et al. Formation of percolating networks in multi-wall carbon-nanotube–epoxy composites. Compos Sci Technol 2004;64(15):2309–16.
[24] Hobbie EK, Fry D. Nonequilibrium phase diagram of sticky nanotube suspensions. Phys Rev Lett 2006;97(3):036101.
[25] Rahatekar SS, Koziol KK, Kline SR, Hobbie EK, Gilman JW, Windle AH. Length-dependent mechanics of carbon-nanotube networks. Adv Mater 2009;21(8):874–8.
[26] Loizou E, Butler P, Porcar L, Kesselman E, Talmon Y, Dundigalla A, et al. Large scale structures in nanocomposite hydrogels. Macromolecules 2005;38(6):2047–9.
[27] Hirschler MM. Use of heat release rate to predict whether individual furnishings would cause self propagating fires. Fire and Safety J 1999;32(3):273–96.